Quantification of oxidative single-base and intrastrand cross-link lesions in unmethylated and CpG-methylated DNA induced by Fenton-type reagents

Huachuan Cao and Yinsheng Wang*

Department of Chemistry-027, University of California, Riverside, CA 92521-0403,USA

ABSTRACT

Methylation of cytosine at CpG sites in mammalian cells plays an important role in the epigenetic regulation of gene expression. Here, we assessed the formation of single-nucleobase lesions and intrastrand cross-link lesions (i.e. G[8-5]C, C[5-8]G, mC[5m-8]G, and G[8-5m]mC, where 'mC' represents 5-methylcytosine) in unmethylated and the corresponding CpG-methylated synthetic double-stranded DNA upon treatment with Fenton-type reagents [i.e. H_2O_2, ascorbate together with Cu(II) or Fe(II)]. Our results showed that the yields of oxidative single-nucleobase lesions were considerably higher than those of the intrastrand cross-link lesions. Although no significant differences were found for the yields of single-base lesions induced from cytosine and mC, the G[8-5m]mC cross-link was induced ~10 times more efficiently than the G[8-5]C cross-link. In addition, the mC[5m-8]G was induced at a level that was ~15 times less than G[8-5m]mC, whereas the corresponding C[5-8]G intrastrand cross-link lesion was not detectable. Moreover, Cu(II) is ~10-fold as effective as Fe(II) in inducing oxidative DNA lesions. These results suggest that oxidative intrastrand cross-link lesions formed at methylated-CpG sites may account for the previously reported mCG→TT tandem double mutations induced by Fenton-type reagents.

INTRODUCTION

Reactive oxygen species (ROS) are produced endogenously, during normal aerobic metabolism and under various pathological conditions, and exogenously, such as upon exposure to UV light, ionizing radiation, environmental mutagens and carcinogens. DNA is susceptible to damage by ROS, and the accumulation of oxidative DNA lesions is associated with aging and a variety of human diseases, including cancer and neurodegeneration (1,2).

A large number of single-nucleobase lesions induced by ROS have been widely studied for their formation, mutagenesis and repair (2,3). Most common point mutations induced by ROS are C→T transitions, suggesting that modified cytosine derivatives are among the most abundant and mutagenic oxidative DNA lesions (4–6). In mammalian cells, cytosines at CpG sites are frequently methylated at the C5 carbon to form 5-methylcytosine (mC), which accounts for ~4% of all dC residues in humans (7,8). The methylated CpGs are mutational hot spots in human *p53* tumor suppressor gene, and the most common mutation is mC→T transition (9).

Pfeifer and coworkers (10) recently observed unusual mCG→TT tandem mutations when CpG-methylated pSP189 plasmid was treated with Cu(II)/H_2O_2/ascorbate and replicated in nucleotide excision repair (NER)-deficient human XPA cells, suggesting that vicinal base damages or intrastrand cross-link lesions formed at methylated CpG dinucleotide sites might be involved. In this context, we previously identified the mC[5m-8]G and G[8-5m]mC cross-link lesions (structures shown in Scheme 1), where the methyl carbon of mC and the C8 of its adjacent guanine are covalently bonded, in oligodeoxyribonucleotides (ODNs) upon exposure to γ rays under aerobic and anaerobic conditions (11,12). Along this line, C[5-8]G and G[8-5]C (Scheme 1) cross-link lesions, where the C5 carbon of cytosine is coupled with the C8 carbon of its neighboring guanine, can also be induced in aqueous solutions of synthetic ODNs exposed to γ- or X-rays (13,14).

Others (14–17) and we (11–13,18,19) demonstrated that intrastrand cross-link lesions could be initiated from a single radical of pyrimidine bases. However, the same radical is also able to couple readily with molecular

*To whom correspondence should be addressed. Tel: +1 951 827 2700; Fax: +1 951 827 4713; Email: yinsheng.wang@ucr.edu.
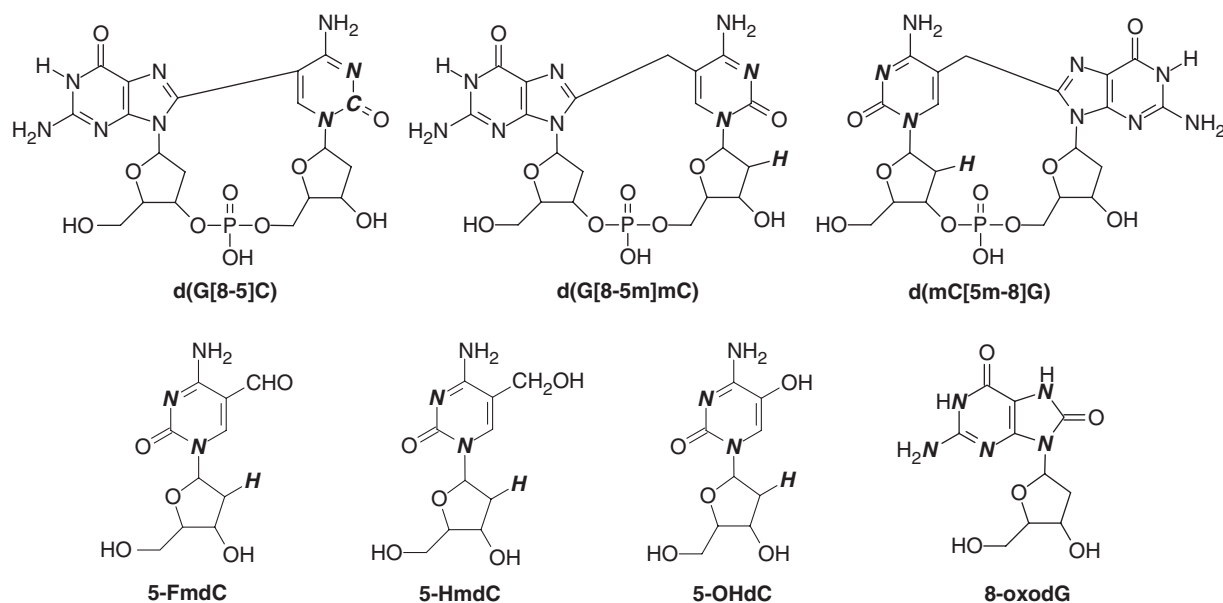
Scheme 1. The structures of isotope-labeled single-nucleobase and intrastrand cross-link lesions employed in this study. (The atoms in bold italic font represent the sites where the stable isotopes were incorporated).
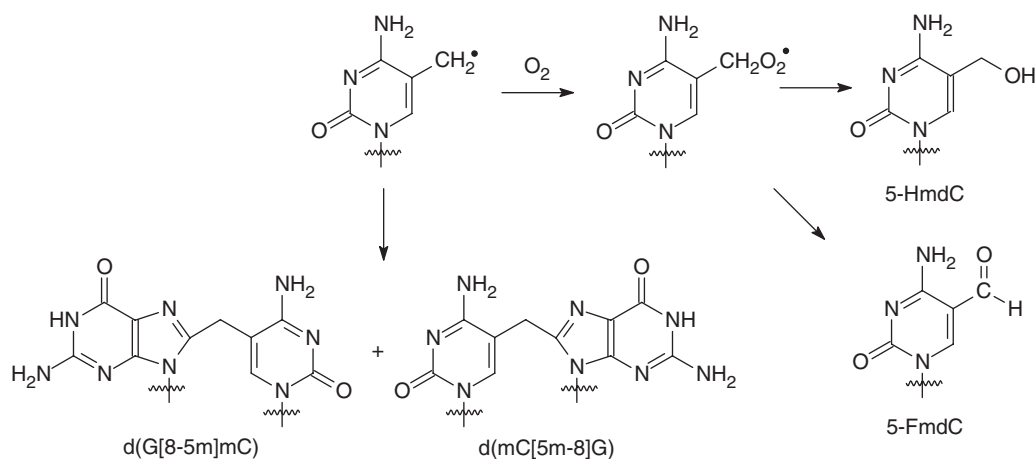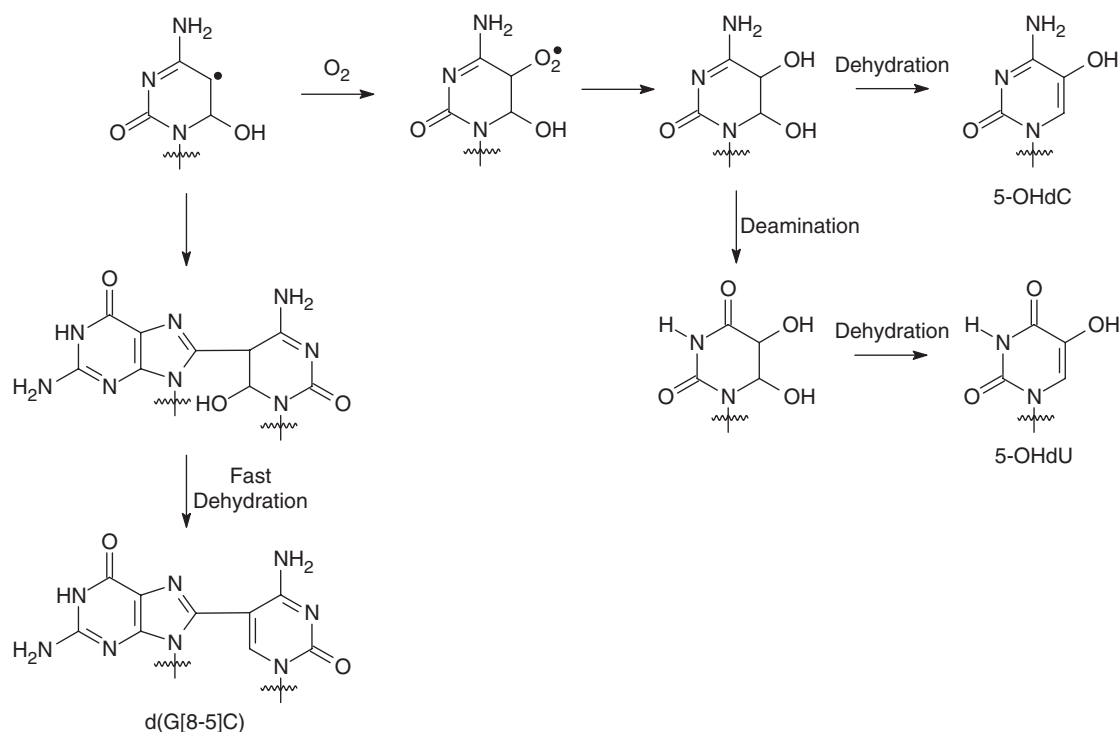

Scheme 2. Generation of single-base and cross-link lesions from the methyl radical of 5-methyl-2′-deoxycytidine.

oxygen and the resulting peroxyl radical can be transformed to give single-nucleobase lesions. For instance, 5-formyl-2′-deoxycytidine (5-FmdC) and 5-hydroxymethyl-2′-deoxycytidine (5-HmdC) can form from the methyl radical of 5-methyl-2′-deoxycytidine (Scheme 2). Likewise, 5-hydroxy-2′-deoxycytidine (5-OHdC) can be induced from the 6-hydroxy-5-yl radical of 2′-deoxycytidine (Scheme 3). The quantification of intrastrand cross-link and single-nucleobase lesions initiated from the aforementioned radials under aerobic conditions can allow for the assessment of the relative contributions of these two pathways, i.e. coupling with O_2 or with its vicinal guanine base. Furthermore, it is important to compare the profiles of oxidative lesions formed in methylated and unmethylated sequences, which may offer insights into understanding the

ubiquitous C→T and the unusual mCG→TT mutations found at CpG sites (9,10).

Hydrogen peroxide (H_2O_2) is produced by endogenous metabolic processes, and it can lead to the formation of hydroxyl radical in the presence of transition metal ions in their reduced states, e.g. Fe(II) or Cu(I). In this context, copper binds to DNA with high affinity to G:C base pairs (20), and it plays a pivotal role in maintaining the structure and integrity of chromatin (21). Cu(II) and H_2O_2, often with the addition of ascorbic acid, can result in the formation of highly reactive species and produce extensive strand breaks (22) as well as many types of single-base lesions in DNA (23), which was found to be enhanced while DNA was packed into nucleosomes (24). It was proposed that free copper ion primarily mediates the formation of frank strand breaks, whereas

Scheme 3. Generation of single-base and cross-link lesions from 6-hydroxy-5-yl radical of 2′-deoxycytidine.

DNA-bound copper induces mainly nucleobase modifications through the formation of DNA–Cu(I)–H$_2$O$_2$ complexes (22,25).

Iron is another biologically relevant transition metal. *In vitro* studies showed that Fe(III)-dependent DNA fragmentation is much less extensive than that produced by equivalent amount of Cu(II) ions under otherwise comparable reaction conditions (26), and Fe(II) induces significantly less nucleobase damage in the presence of H$_2$O$_2$ than does Cu(II) (23,27). On the other hand, studies with Jurkat cells revealed that intracellular iron, but not copper, plays an important role in H$_2$O$_2$-mediated formation of strand breaks in DNA (28).

Although the structures of various single-nucleobase lesions induced by Fenton reactions have been well established, there were few reports on the formation of cross-linked nucleobase lesions from treatment with Fenton-type reagents. In the latter respect, Randerath and others (29–34) detected, by ^{32}P-postlabeling assay, several bulky DNA adducts that are induced endogenously in animal tissues or from the Fenton reaction mixture of synthetic ODNs. On the grounds that some of the bulky adducts were commonly formed in ODNs housing-specific dinucleotide sequences, these authors proposed that these adducts might be intrastrand cross-link lesions (32). These bulky lesions were also found in tissues from animals exposed to pro-oxidant chemicals, which firmly linked the formation of the bulky adducts to ROS (31,35). More recently, Randerath *et al.* (36) demonstrated that some of the bulky DNA adducts actually contained the 8,5′-cyclo-2′-deoxyadenosine (cyclo-dA). The cyclo-dA bears a covalent bond between the C8 of adenine and the C$_{5'}$ carbon in the same nucleoside. There were also indications that intrastrand cross-links might be induced in salmon sperm DNA upon treatment with Fenton-type reagents; the structures of these putative cross-link lesions, however, remain elusive (37,38). Recently, we first reported the formation of a structurally defined G[8-5m]T intrastrand cross-link lesion, which bears a covalent bond between the methyl carbon of thymine and the C8 of its adjacent 5′ guanine, in calf thymus DNA upon treatment with Cu(II)/H$_2$O$_2$/ascorbate (39). It remains to be established whether intrastrand cross-link lesions can also form between guanine and its neighboring cytosine or mC in DNA upon exposure to Fenton-type reagents.

In the present study, we synthesized several isotope-labeled oxidative single-base and cross-link lesions originated from 2′-deoxycytidine (dC) and 5-methyl-2′-deoxycytidine (5-mdC) (Scheme 1), and employed LC-MS/MS with the standard isotope dilution method to identify and quantify the single-nucleobase and intrastrand cross-link lesions formed in synthetic duplex ODNs upon incubation with Cu(II)/H$_2$O$_2$/ascorbate or Fe(II)/H$_2$O$_2$/ascorbate. The results allowed us to compare the reactivities of methylated and unmethylated cytosine residues toward Fenton-type reagents mediated by two different transition metal ions, i.e. iron and copper. Moreover, we demonstrated that G[8-5]C, mC[5m-8]G and G[8-5m]mC cross-link lesions, which were previously shown to be generated upon exposure to γ rays (11–13), could also be induced by Fenton-type reagents.

Table 1. Sequences of ODNs used for treatment with the Fenton-type reagents[a]

ODNs	Sequences[a]
ODN1/2	5′-XGXGXGXGXGXGXGXGXG-3′
ODN3/4	5′-TXGATGXATGXATXGA-3′

[a]ODN1/ODN3, X = C; ODN2/ODN4, X = mC.

EXPERIMENTAL PROCEDURES

Materials

CuCl$_2$, (NH$_4$)$_2$Fe(SO$_4$)$_2$·6H$_2$O, L-methionine, L-ascorbic acid and alkaline phosphatase were from Sigma–Aldrich (St Louis, MO, USA). Hydrogen peroxide (30%) and nuclease P1 were purchased from Fisher Scientific (Fair Lawn, NJ, USA) and MP Biomedicals (Aurora, OH, USA), respectively. Snake venom phosphodiesterase and calf spleen phosphodiesterase were obtained from US Biological (Swampscott, MA, USA). Common reagents for solid-phase DNA synthesis were obtained from Glen Research Co. (Sterling, VA, USA). Unmodified ODNs (Table 1) used in this study were purchased from Integrated DNA Technologies (Coralville, IA, USA) and purified by HPLC. [2-amino-1,3,7,9–$^{15}N_5$]-8-oxo-2′-deoxyguanosine was synthesized as described previously (39).

Synthesis and characterization of compounds

Scheme 1 depicts the structures of the lesions that we quantified in this study. The sites of isotope incorporation are indicated by bold italic font, in which the nitrogen, carbon and hydrogen atoms were replaced with ^{15}N, ^{13}C and deuterium, respectively. The labeled and unlabeled single-nucleobase lesions were prepared according to previously described procedures (40).

[1,3-$^{15}N_2$-2′-D]-5-hydroxymethyl-2′-deoxyuridine (Compound 1 in Scheme S1). This compound was synthesized using the multi-step procedures reported by Sowers *et al.* (40).

Compounds 2–5 (Scheme S1). These four compounds were prepared following the previously described methods for the preparation of the unlabeled compounds (11) and the NMR data for labeled compounds **2–4** were reported earlier (39).

Compound 5. Yield 85%. ESI-MS: *m/z* 907.5 [M + H]$^+$. ^{31}P NMR (CDCl$_3$): δ 150.58, 149.87.

Isotope-labeled d(G[8-5m]mC) and d(mC[5m-8]G). With compound **5**, we synthesized a dinucleoside monophosphate d(XG) and an ODN d(CCGXCCGG), where 'X' represents the isotope-incorporated 4-(1,2,4-triazol-1-yl)-5-phenylthiomethyl-2′-deoxyuridine, on a Beckman Oligo 1000S DNA synthesizer (Fullerton, CA, USA) at 1-μmol scale. The deprotection of the synthetic product was carried out by treatment with concentrated ammonia at room temperature for 48 h, during which 1,2,4-triazol-1-yl

Table 2. Concentrations of Fenton-type reagents employed for the treatment of DNA[a]

	Control	A	B	C	D	E
Cu(II)/Fe(II) (μM)	100	6.75	12.5	25	50	100
H$_2$O$_2$ (μM)	0	50	100	200	400	800
Ascorbate (mM)	0	0.5	1.0	2.0	4.0	8.0

[a]All reactions were carried out in a 100-μl solution containing 5 nmol ODNs in 25 mM NaCl and 50 mM phosphate (pH 7.0).

group was converted to an amino group and yielded the desired radical precursor 5-(phenylthiomethyl)-2′-dC. The ODN was further purified and desalted by using HPLC (HPLC section; ESI-MS and MS/MS results for this ODN are shown in Figure S3). An aqueous solution of the ODN with an OD260 of 0.4 was dispersed in a quartz tube, degassed by bubbling with argon for 30 min and irradiated with 254-nm UV light from a TLC lamp (UVGL-58, UVP Inc., Upland, CA, USA) at room temperature for 20–25 min with continuous argon bubbling. The solution was dried in a Speed-Vac and reconstituted in water for digestion with a combination of four enzymes (*vide infra*), and the digestion mixture was separated by HPLC to obtain the isotope-labeled d(G[8-5m]mC) (Figures S1 and S2). Dinucleoside monophosphate d(XG) was irradiated under the similar conditions as described above, and the irradiation mixture was separated by HPLC to render the isotope-labeled d(mC[5m-8]G).

Quantification of standard DNA lesions

The concentrations of stock solutions of 5-FmdC, 5-HmdC, 5-OHdC, 8-oxodG, d(G[8-5m]mC) and d(G[8-5]C) were determined by UV absorbance measurements. The molar extinction coefficients (in l/mol/cm) used to quantify the standard solutions were: 5-FmdC, ε_{283} = 13 700; 5-HmdC, ε_{274} = 9070; 5-OHdC, ε_{292} = 6025 (4); 8-oxodG, ε_{294} = 9700 (41); d(G[8-5m]mC), ε_{260} = 23 800 and d(G[8-5]C), ε_{260} = 22 800 (42). The ε values for 5-FmdC, 5-HmdC and d(G[8-5m]mC) were determined by ^{1}H-NMR (Figures S4–S6) following the previously described method (43).

Treatment of synthetic ODNs with Fenton-type reagents

The ODNs were annealed in a buffer containing 50 mM NaCl and 20 mM phosphate (pH 6.9) by heating the solution to 90°C and cooling slowly to room temperature. Aliquots of ODNs (5 nmol) were incubated with CuCl$_2$ or (NH$_4$)$_2$Fe(SO$_4$)$_2$ (6.25–100 μM), H$_2$O$_2$ (50–800 μM) and ascorbate (0.5–8 mM) in a 100-μl solution containing 25 mM NaCl and 50 mM phosphate (pH 7.0) at room temperature for 60 min. All chemicals were freshly dissolved in doubly distilled water and the reactions were carried out under aerobic conditions. The detailed concentrations of individual Fenton-type reagents used for the reactions were shown in Table 2. The reactions were terminated by adding an excess amount of L-methionine, and the ODN samples were desalted by ethanol precipitation.

Control experiments were also carried out to examine the effect of individual components in Fenton-type system on the formation of DNA lesions. First, we incubated ODNs with 200 μM H_2O_2 and 2 mM ascorbate in the absence of Cu(II) or Fe(II). Second, ODNs were incubated with 25 μM $CuCl_2$ or $(NH_4)_2Fe(SO_4)_2$ and 200 μM H_2O_2, and no ascorbate was added. In addition, experiments were carried out in the presence of 4 mM dimethyl sulfoxide (DMSO), a hydroxyl radical scavenger, for Fenton reaction condition C (Table 2).

Enzymatic digestion of DNA

Four units of nuclease P1, 0.005 unit of calf spleen phosphodiesterase, and 1.5 μl solution containing 300 mM sodium acetate (pH 5.0) and 10 mM zinc acetate were added to 15 μl ODN samples treated with Fenton-type reagent, and the digestion was carried out at 37°C for 6 h. To the digestion mixture were then added 10 U of alkaline phosphatase, 0.05 U of snake venom phosphodiesterase and 5 μl of 0.5 M Tris–HCl buffer (pH 8.9). The digestion was continued at 37°C for 6 h, and the enzymes were removed by passing through a 10-kDa cutoff Centricon membrane (Millipore, Billerica, MA). The amount of nucleosides in the mixture was quantified by UV absorbance measurements, and to the mixture were then added isotope-labeled standard lesions. The resulting aliquots were subsequently subjected to HPLC enrichment and LC-MS/MS analysis.

HPLC

Off-line HPLC separation was preformed on a system composed of a Hitachi L-6200A pump (Hitachi Ltd, Tokyo, Japan), an HP-1050 UV detector (Agilent Technologies, Palo Alto, CA, USA) and a Peak Simple Chromatography Data System (SRI Instruments Inc., Las Vegas, NV, USA). A 4.6 × 250 mm Apollo C18 column (5 μm in particle size, 300 Å in pore size, Alltech Associates Inc., Deerfield, IL, USA) was used for the separation of synthetic ODNs and the enzymatic digestion products of the UV irradiation mixture of the d(CCGXCCGG) and d(XG). The flow rate was 0.8 ml/min. For the ODN separation, a solution of 50 mM triethylammonium acetate (TEAA, pH 6.6, solution A) and a mixture of 50 mM TEAA and acetonitrile (70/30, v/v) (solution B) were used as mobile phases. A gradient of 5 min 0–20% B, 45 min 20–50% B and 5 min 50–100% B was employed. The separation of the enzymatic digestion products of 8-mer irradiation mixture or the irradiation mixture of d(XG) was carried out by using 10 mM ammonium formate (solution A) and 30% acetonitrile in 10 mM ammonium formate (solution B) as mobile phases, and the gradient was 20 min 0–20% B, 30 min 20–35% B followed by 15 min 35–100% B.

The enrichment of DNA lesions from the digestion mixture of Fenton-type reagent-treated ODNs was performed on a Surveyor HPLC system (Thermo Fisher Scientific, Waltham, MA, USA) equipped with a 4.6 × 150 mm Zorbax SB-AQ reverse phase C18 column (5 μm in particle size, Agilent Technologies). A gradient of 40 min 0–25% acetonitrile in 10 mM ammonium formate (pH 6.3) was employed, and the flow rate was 0.60 ml/min. We collected fractions in a wide retention time range (3–4 min) to ensure that the lesions were completely collected while the unmodified nucleosides were excluded as much as possible. The collected fractions were dried in a Speed-vac, and re-dissolved in 10 μl of H_2O for LC-MS/MS analysis.

LC-MS/MS analysis

On-line HPLC–MS/MS measurements were carried out using an Agilent 1100 capillary HPLC pump (Agilent Technologies) and an LTQ linear ion-trap mass spectrometer (Thermo Fisher Scientific), which was set up for monitoring the fragmentation of the $[M + H]^+$ ions of the labeled and unlabeled single-base or cross-link lesions. A 0.5 × 150 mm Zorbax SB-C18 column (particle size 5 μm, Agilent Technologies) was used for the separation of the DNA hydrolysis samples, and the flow rate was 6.0 μl/min. A 60-min gradient of 0–25% acetonitrile in 20 mM ammonium acetate was employed for the analysis of HPLC-enriched oxidative lesions.

RESULTS

LC-MS/MS identification and quantification of DNA lesions formed in ODNs 1 and 2 induced by Cu(II)/H_2O_2/ascorbate

We annealed separately the self-complementary ODNs 1 and 2 (Table 1) to form duplexes and treated them with different concentrations of Cu(II)/H_2O_2/ascorbate (Table 2), digested the resulting DNA samples with enzymes, and analyzed the digestion mixtures by LC-MS/MS with stable isotope-labeled lesions as internal standards.

The selected-ion chromatogram (SIC) for the m/z 569→275 transition, which monitors the loss of 2-deoxyribose/phosphate backbone, showed a fraction eluting at the same time as the labeled d(G[8-5m]mC) internal standard (Figure 1a and b; the sample was from ODN2 treated under condition C listed in Table 2). Similarly, the SIC for m/z 569→275 transition, which showed a peak at the same retention time as the labeled d(mC[5m-8]G) at around 13 min, supported the formation of d(mC[5m-8]G) (Figure 1c and d). The product-ion spectrum of the ion of m/z 569 further revealed the presence of d(G[8-5m]mC) and d(mC[5m-8]G) in the enzymatic digestion mixture of the treated ODNs (Figure 1). Moreover, the amounts of d(G[8-5m]mC) and d(mC[5m-8]G) are significantly lower in the control samples without hydrogen peroxide treatment, showing that the G[8-5m]mC and mC[5m-8]G intrastrand cross-link lesions can indeed be induced by Fenton-type reagents. In this regard, our previous studies revealed that G[8-5m]mC and mC[5m-8]G could be initiated from the 5-(2′-deoxycytidinyl)methyl radical (11,12), which can result from the ·OH-mediated hydrogen abstraction from the methyl group of mC (Schemes 1 and 2) (44).

We also observed the formation of d(G[8-5]C) cross-link based on the peak at 20.8 min found in the SIC for the m/z 555→457 transition (Figure 2). This component co-elutes with the isotope-labeled internal standard
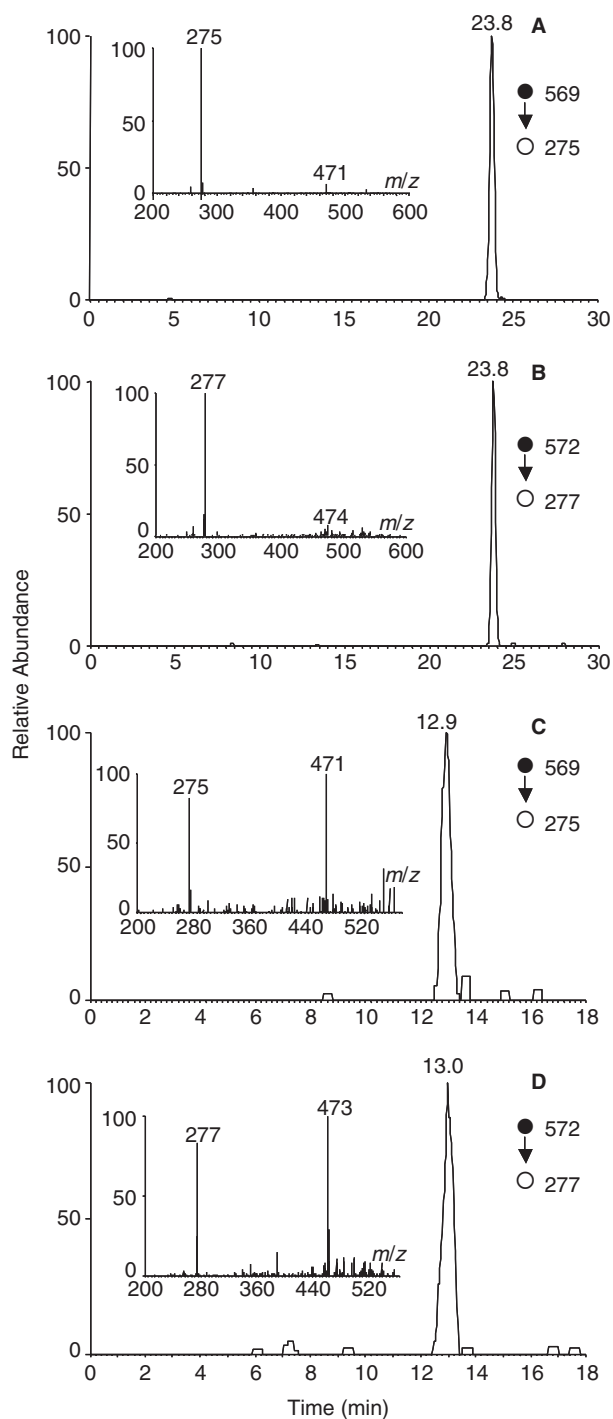
Figure 1. Selected-ion chromatograms (SICs) for the monitoring of the *m/z* 569→275 [**A**, for unlabeled d(G[8-5m]mC)], *m/z* 572→277 [**B**, for labeled d(G[8-5m]mC)], *m/z* 569→275 [**C**, for unlabeled d(mC[5m-8]G)] and *m/z* 572→277 [**D**, for labeled d(mC[5m-8]G)] transitions in Cu(II)/ H₂O₂/ascorbate-treated ODN2 under reaction condition C (Table 2). Shown in the insets are the product-ion spectra of the [M + H]⁺ ions of the unlabeled and labeled d(G[8-5m]mC) and d(mC[5m-8]G).

of d(G[8-5]C). Furthermore, the relative abundances of the two major fragment ions formed from the cleavage of the ion of *m/z* 555 match those formed from the fragment-ation of the [M + H]⁺ ion of the internal standard, further supporting the presence of d(G[8-5]C) in the
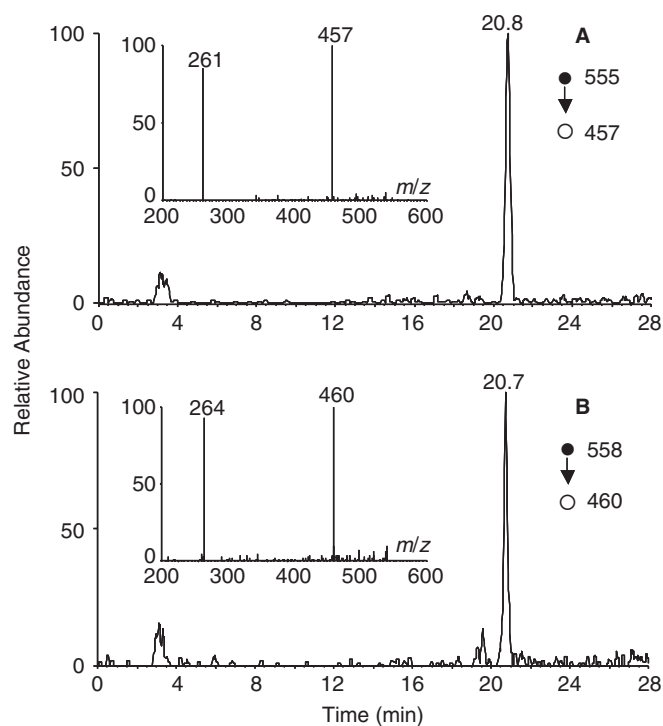

Figure 2. SICs for the monitoring of the *m/z* 555→457 [**A**, for unlabeled d(G[8-5]C)] and *m/z* 558→460 [**B**, for labeled d(G[8-5]C)] transitions in Cu(II)/H₂O₂/ascorbate-treated ODN1 under reaction condition C (Table 2). Shown in the insets are the product-ion spectra of the [M + H]⁺ ions of the unlabeled and labeled d(G[8-5]C).

enzymatic digestion mixture of ODN1 after treatment with Fenton-type reagents (Figure 2). It is worth noting that we attempted, but failed to detect the d(C[5-8]G) in the enzymatic digestion mixture. The formation of G[8-5m]mC, mC[5m-8]G and G[8-5]C intrastrand cross-link lesions exhibited linear dose-dependent increase when the concentrations of H₂O₂ were up to 800 μM; however, the yield of G[8-5m]mC is ~13 and 16 times greater than those of G[8-5]C and mC[5m-8]G, respectively, upon treatment with the same dose of Cu(II)/H₂O₂/ascorbate (Figure 3, and calibration curves for LC-MS/MS quanti-fication are shown in Figure S12).

Previously we demonstrated that the yields of mC[5m-8]G and G[8-5m]mC are much higher under anaerobic than aerobic conditions, suggesting the compe-tition between coupling with molecular oxygen and conju-gating with its neighboring base (12). Given that ·OH can also result in the formation of single-base lesions under the same oxidation conditions, it is important to examine the formation of these lesions. Not surprisingly, LC-MS/MS analysis also confirmed the formation of 5-FmdC and 5-HmdC in ODN2 (Figures S7 and S8) and 5-OHdC in ODN1 upon treatment with Fenton-type reagents (Figure S9). The quantification results showed that, at doses up to 800 μM H₂O₂ and 100 μM Cu(II) (Table 2), the yields of the lesions increased proportionally with the rise in the concentrations of the Fenton-type reagents. Moreover, the yields of single-base lesions were 2–3 orders of magnitude higher than those of the cross-link lesions (Figure 3).
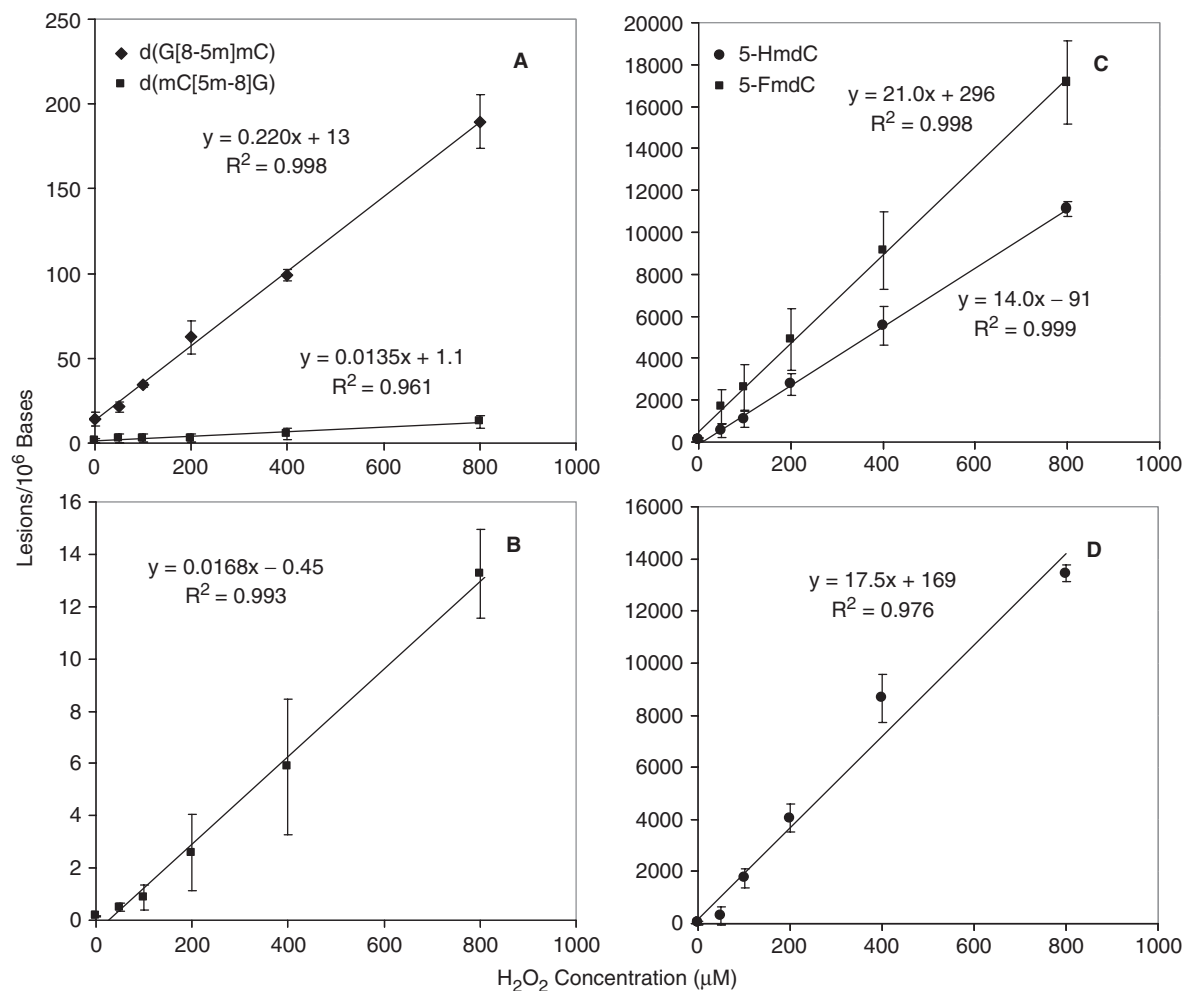
Figure 3. Cu(II)/H₂O₂/ascorbate-induced formation of single-base and cross-link lesions in ODNs 1 and 2: (**A**) d(G[8-5m]mC) (filled diamond) and d(mC[5m-8]G) (filled square); (**B**) d(G[8-5]C)(filled square); (**C**) 5-HmdC (filled circle) and 5-FmdC (filled square) and (**D**) 5-OHdC (filled circle). The values represent the means ±SD from three independent oxidation and quantification experiments.

LC-MS/MS identification and quantification of DNA lesions formed in ODNs 1 and 2 upon Fe(II)/H₂O₂/ascorbate treatment

Iron is another biologically important transition metal which can participate in Fenton-type reactions. To assess the different effects of iron and copper on inducing oxidative DNA lesions, we also examined DNA lesions produced in ODNs 1 and 2 upon treatment with Fe(II)/H₂O₂/ascorbate. It turned out that the yields of cross-link and single-base lesions were markedly lower when Cu(II) was replaced with Fe(II) under otherwise identical experimental conditions (Figures 3 and 4). In addition, the amounts of d(mC[5m-8]G), d(C[5-8]G) and d(G[8-5]C) induced in ODNs 1 and 2 were below the detection limits of our LC-MS/MS method. Furthermore, the yields of 5-HmdC, 5-FmdC and d(G[8-5m]mC) rise proportionally with the increase of the concentration of Fenton-type reagents; however, the amount of 5-OHdC exhibited a slightly different trend. The yields of 5-OHdC at low-dose range increased linearly with the rise in the concentrations of Fenton-type reagents. On the other hand, when the

DNA was treated with the highest dose of Fe(II)/H₂O₂/ascorbate ([H₂O₂] = 800 μM), the yield of 5-OHdC increased considerably, which was 10-fold higher than the yield found at the second highest dose ([H₂O₂] = 400 μM, Figure 4C). The exact reason for the disproportionally high yield found at the highest dose is not clear, though we suspect that the duplex DNA may undergo a conformational change at this high concentration of Fe(II).

LC-MS/MS quantification of DNA lesions formed in ODNs 3 and 4 oxidized with Cu(II)/H₂O₂/ascorbate

It is known that the methylation in poly(GC) sequence can facilitate the conformational change of DNA, most notably the transition from normal B to Z-form DNA in the presence of divalent metal ions (45). Therefore, we also treated two mixed-sequence ODNs (ODNs 3 and 4 in Table 1), which contain both the GX and XG sites (X = C or mC), with Cu(II)/H₂O₂/ascorbate at the two highest doses. It turned out that the yields of oxidative lesions are comparable with what we found for ODN1 and
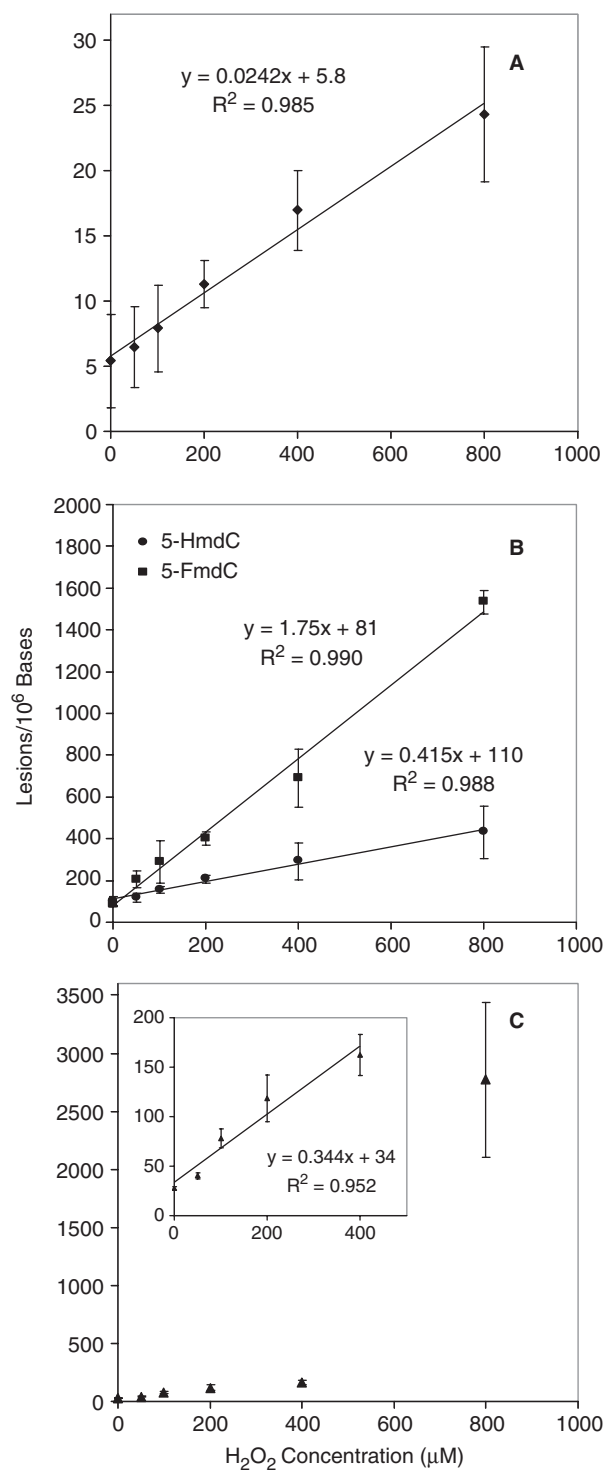
Figure 4. Fe(II)/H$_2$O$_2$/ascorbate-induced formation of single-base and cross-link lesions in ODNs 1 and 2: (**A**) d(G[8-5m]mC) (filled diamond); (**B**) 5-HmdC (filled circle) and 5-FmdC (filled square) and (**C**) 5-OHdC (filled triangle). The values represent the means ±SD from three independent oxidation and quantification experiments.

Figure 5. Cu(II)/H$_2$O$_2$/ascorbate-induced formation of single-base and cross-link lesions in ODNs 3 and 4: (**A**) 5-FmdC, 5-HmdC and 8-oxodG; (**B**) 5-OHdC and 8-oxodG; (**C**) d(G[8-5m]mC) and d(G[8-5]C). The values represent the means ±SD from three independent oxidation and quantification experiments. The concentrations of H$_2$O$_2$ were 0 (control), 400 (condition D) and 800 μM (condition E, Table 2), respectively.

ODN2 (Figure 5). In addition, we quantified the yield of 8-oxo-7,8-dihydro-2′-deoxyguanosine (8-oxodG, Figures S10 and S11), an abundant and well-studied oxidativ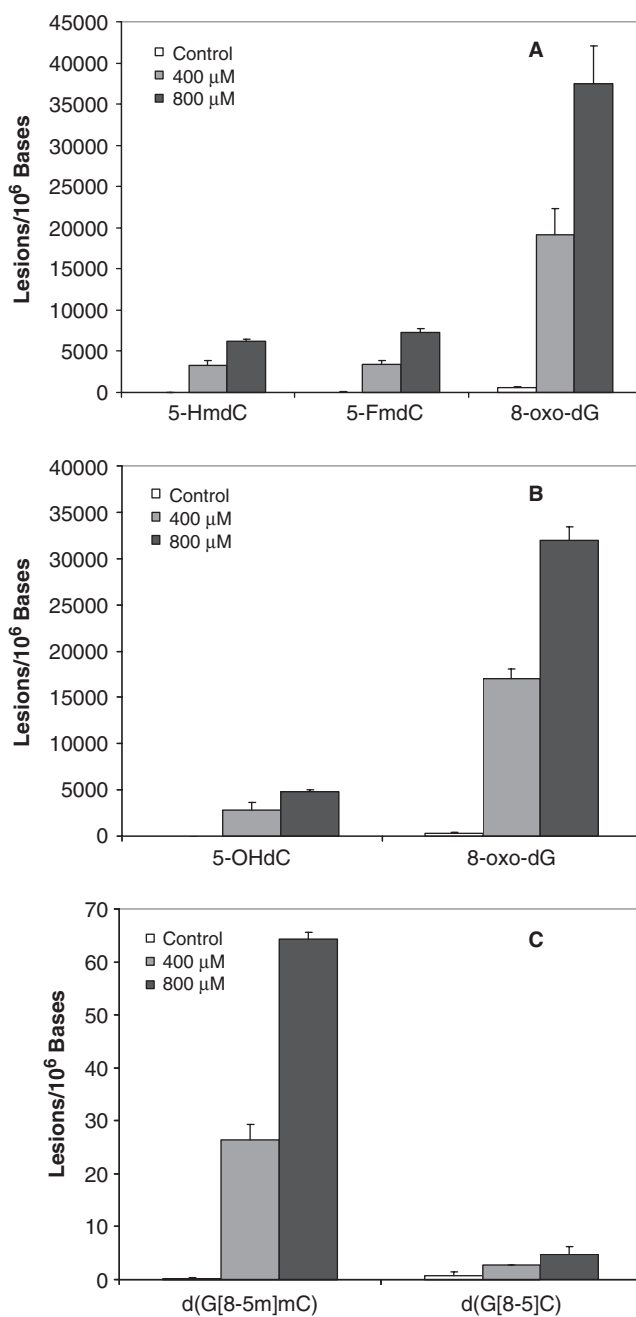e DNA lesion. Our results showed that the amount of 5-HmdC, 5-FmdC or 5-OHdC was 4–6-fold lower than that of 8-oxodG (Figure 5a and b).

Effects of individual components in Fenton-type reagents and a radical scavenger DMSO

We also carried out several control experiments to gain insights into the mechanism for the formation of the
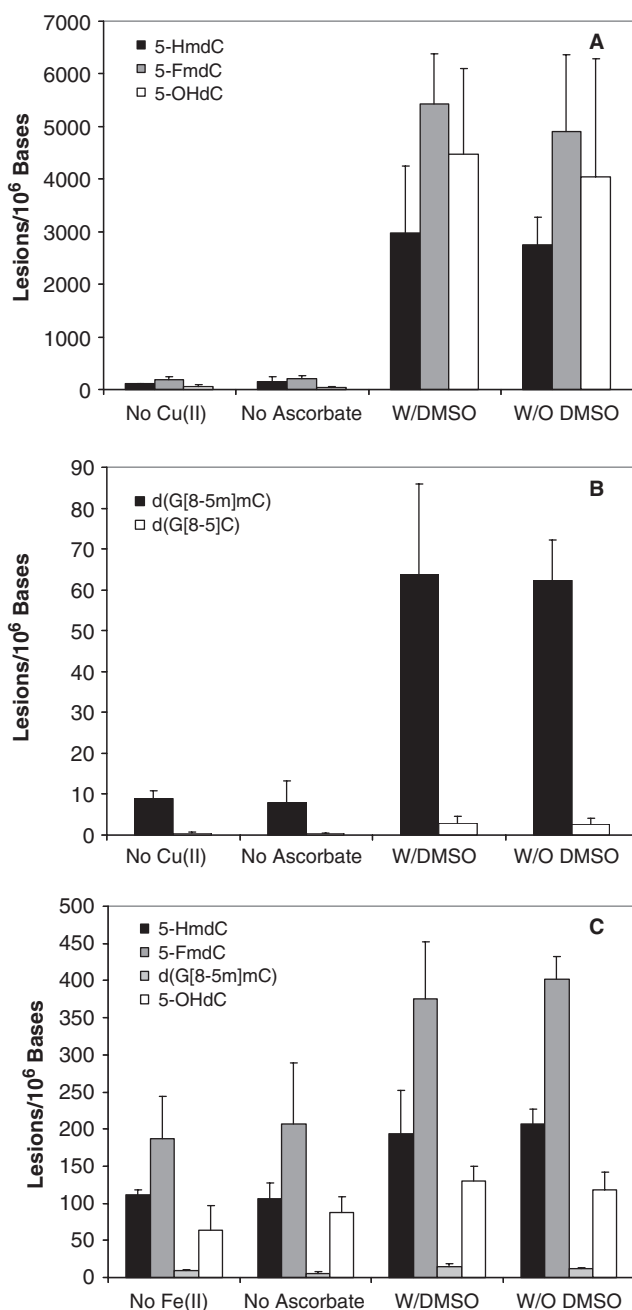
Figure 6. Cu(II)/H$_2$O$_2$/ascorbate and Fe(II)/H$_2$O$_2$/ascorbate-induced formation of single-base and cross-link lesions in ODNs 1 and 2 under different experimental conditions: (**A**) 5-FmdC, 5-HmdC and 5-OHdC induced by Cu(II)/H$_2$O$_2$/ascorbate; (**B**) d(G[8-5m]mC) and d(G[8-5]C) induced by Cu(II)/H$_2$O$_2$/ascorbate; (**C**) 5-FmdC, 5-HmdC, 5-OHdC and d(G[8-5m]mC) induced by Fe(II)/H$_2$O$_2$/ascorbate. 'No Cu(II)'/'No Fe(II)', 200 μM H$_2$O$_2$ and 2 mM ascorbate; 'No Ascorbate', 200 μM H$_2$O$_2$ and 25 μM Cu^{2+}/Fe^{2+}; 'W/DMSO', 200 μM H$_2$O$_2$, 25 μM Cu^{2+}/Fe^{2+}, 2 mM ascorbate and 4 mM DMSO; and 'W/O DMSO', 200 μM H$_2$O$_2$, 25 μM Cu^{2+}/Fe^{2+} and 2 mM ascorbate. The values represent the means ±SD from three independent oxidation and quantification experiments.

oxidative lesions under Fenton-type reaction conditions. In the absence of transition metal ions, the yields of lesions were sharply reduced (Figure 6). Leaving out ascorbate resulted in pronounced decrease in the yields of both

single-base and intrastrand cross-link lesions (Figure 6). However, treatment of duplex DNA with Fe(II)/H$_2$O$_2$ results in the formation of higher levels of lesions than the corresponding treatment with Cu(II)/H$_2$O$_2$ (Figure 6). This observation is in keeping with the fact that Fe(II) can react directly with H$_2$O$_2$ to generate ·OH, whereas Cu(II) has to be reduced by ascorbate to give Cu(I) before it can participate in Fenton-type reaction to afford ·OH.

We also incubated ODNs with Fenton-type reagents in the presence of DMSO, a free ·OH scavenger, and assessed the formation of oxidative DNA lesions under these conditions. It turned out that the presence of DMSO does not result in obvious decrease in the yields of single-base and cross-link lesions. This result suggests that the DNA-bound metal ions induce site-specific formation of ·OH, which cannot be intercepted by the radical quencher DMSO. The resulting nucleobase radical can then couple with either molecular oxygen and its neighboring nucleobase to form single-base and intrastrand cross-link lesions, respectively.

DISCUSSION

Here we demonstrated, by using LC-MS/MS with the standard isotope dilution method, that the treatment of duplex ODNs with Cu(II)/H$_2$O$_2$/ascorbate can lead to the formation of G[8-5]C, mC[5m-8]G and G[8-5m]mC. Quantification results revealed that the yields of G[8-5]C and mC[5m-8]G cross-links (Figure 3a and b) are comparable with what we reported for another intrastrand cross-link, G[8-5m]T, in calf thymus DNA treated with the similar doses of Cu(II)/H$_2$O$_2$/ascorbate (39). In contrast, the C[5-8]G lesion was below the detection limit of our LC-MS/MS method. The yield of G[8-5m]mC formed in methylated duplex ODNs is, however, 13-fold greater than that of G[8-5]C produced in unmethylated ODNs under the same oxidation conditions (Figure 3a and b). Together, these data support that, upon treatment with Fenton-type reagents, the formation of intrastrand cross-link between guanine and its neighboring mC occurs at a much greater efficiency than that between guanine and its neighboring unmethylated cytosine. Our results also revealed that Cu(II)/H$_2$O$_2$/ascorbate system is ~10 times as effective as Fe(II)/H$_2$O$_2$/ascorbate system in inducing these cross-link lesions.

Previous studies demonstrated that G[8-5]C, G[8-5m]T and G[8-5m]mC cross-link lesions reduced the stability of duplex DNA (46,47), and the former two lesions blocked DNA synthesis by replicative DNA polymerases (46,48). Moreover, G[8-5]C could be bypassed by yeast pol η, a translesion synthesis DNA polymerase, with reduced efficiency and fidelity of nucleotide incorporation at the site opposite the 5′ guanine moiety of the lesion (13). Recent *in vitro* repair studies revealed that both G[8-5]C and G[8-5m]mC could be recognized and incised by *Escherichia coli* UvrABC nucleases (47), suggesting that oxidative intrastrand lesions might be substrates for NER enzymes *in vivo*. Furthermore, we found that G[8-5m]mC-bearing substrates could be incised by UvrABC nuclease with lower efficiency than the

corresponding G[8-5]C-containing duplex (47). The poorer repair and more efficient formation of intrastrand cross-link lesion at GmC than at GC site may lead to the accumulation of such lesions and contribute to increased mutation rate at methylated CpG sites. The formation of the intrastrand cross-link lesions, proposed to be substrates for NER pathway (47,49,50), may pose a risk for people with diseases associated with defects in NER, e.g. *Xeroderma pigmentosum* (XP) (51). Future studies on intrastrand cross-link lesions reported here may contribute to a better understanding of pathological symptoms associated with NER-deficient diseases.

Pfeifer *et al.* (10) recently found an unusually high frequency of mCG→TT tandem double mutation when $Cu(II)/H_2O_2$/ascorbate-treated, CpG-methylated pSP189 shuttle vector was replicated in NER-deficient XPA cells. The corresponding CG→TT mutation occurred at a much lower frequency when the corresponding unmethylated vector was treated with $Cu(II)/H_2O_2$/ascorbate and propagated in the same cell line. These authors proposed that vicinal or cross-linked base damage originated from mC and its neighboring guanine might be involved (10). Quantification data presented in this study support that intrastrand cross-link lesion formed between mC and its adjacent guanine might contribute to such tandem base substitutions since the mC[5m-8]G cross-link lesion was observed, whereas the C[5-8]G cross-link was not detectable. Along this line, if a guanine is situated on the 5′ side of mCpG sites, the yield of G[8-5m]mC cross-link lesion is dramatically enhanced, by more than 10-fold, compared with corresponding G[8-5]C induced at the unmethylated CpG sites.

For comparison, we also quantified the single-base lesions induced by the Fenton-type reagents under the same experimental conditions. It turned out that the yields for these single-base lesions were 2–3 orders of magnitude greater than those of intrastrand cross-link lesions formed at GC, mCG or GmC site (Figures 3–5). These results indicate that the addition of molecular oxygen to pyrimidine radicals is much more facile than the coupling of the pyrimidine radicals to their adjacent purine bases.

Quantification results also showed that 5-OHdC is induced at a similar efficiency as 5-HmdC and 5-FmdC regardless of the sequences of ODNs and the types of transition metal ions being Cu(II) or Fe(II), whereas 5-hydroxy-2′-deoxyuridine (5-OHdU) is below the detection limit of our LC-MS/MS method, particularly at lower doses. The hydroxyl radical couples preferentially to the C5=C6 double bond in cytosine, which can lead to the formation of cytosine glycol. Cytosine glycol can undergo facile dehydration to yield 5-OHdC or undergo both deamination and dehydration to give 5-OHdU (Scheme 3) (52).

Similar addition of hydroxyl radical to the C5=C6 double bond of mC can lead to the formation of mC glycol, which can deaminate to give thymine glycol (53,54). Because of the lack of isotope-labeled internal standards of thymidine glycol, the formation of this lesion from the mC-bearing strand was not quantified in the present study. In addition, the hydroxyl radical can abstract a hydrogen atom from the methyl group of mC

to give the methyl radical of the pyrimidine base, which can further transform to give 5-HmdC and 5-FmdC under aerobic conditions (54). With the above quantification results, it is reasonable to speculate that the total amount of hydroxyl radical-induced major single-base lesions from mC can be several fold higher than those formed from unmethylated cytosine. The more facile formation of single-base lesion at mC than at unmethylated cytosine may account for the prevalent C→T transition mutation found at CpG site in human *p53* gene, and mutation in *p53* is a hallmark for many types of human tumors (55). In this context, both 5-OHdC and 5-FmdC were found to be mutagenic *in vivo*; a mutation frequency of 0.05% was reported for the former after 5-OHdC-bearing single-stranded M13 genome was propagated in *E. coli* cells (5), and a mutation frequency of 0.03–0.28% was found for the latter after the 5-FmdC-carrying double-stranded shuttle vectors were replicated in simian COS-7 cells (56). To our knowledge, the mutagenic properties of 5-HmdC have not yet been examined.

The methylation pattern of cytosine residues at CpG sites and post-translational modifications of histones are crucial for maintaining the epigenetic code in human cells (57). The modification at CpG sequence can result in disturbed gene regulation and heritable epigenetic changes in chromatin. Recent studies revealed that the presence of 8-oxodG or 5-HmdC at CpG site reduced significantly the binding of DNA to methyl-CpG-binding proteins by at least 10-fold (58). These lesions also alter the site selectivity of cytosine methylation at CpG site induced by human maintenance DNA methyltransferase DNMT1 (59,60). High yield of 8-oxodG, 5-HmdC and 5-FmdC observed in our experiment (Figures 3–5) may indicate that DNA damage-mediated alteration in methylation pattern and subsequent binding by methyl-CpG-binding proteins can be significant *in vivo*.

The intracellular concentrations of iron and copper ions can be dramatically increased under oxidative stress conditions through their release from the iron- or copper-storage proteins (61,62). In humans, genetic hemochromatosis and Wilson's disease cause abnormal accumulation of iron and copper, respectively, in various organs. An accumulation of highly mutagenic oxidative lesions in genomic DNA has been considered to be relevant to iron-induced carcinogenesis in iron-overload diseases (63,64). Bulky DNA lesions were found in the liver of patients with Wilson's disease and primary hemochromatosis (65). Our current results support the argument that transition metal ions, especially copper, can induce significant amount of DNA damage, including bulky intrastrand cross-link lesions, in the presence of antioxidant such as ascorbate, which reduces the high-valence Cu^{2+}/Fe^{3+} so as to generate hydroxyl radical via the Fenton-type reaction.

SUPPLEMENTARY DATA

Supplementary Data are available at NAR Online.

ACKNOWLEDGEMENT

REFERENCES

1. Finkel,T. and Holbrook,N.J. (2000) Oxidants, oxidative stress and the biology of ageing. *Nature*, **408**, 239–247.
2. Cooke,M.S., Evans,M.D., Dizdaroglu,M. and Lunec,J. (2003) Oxidative DNA damage: mechanisms, mutation, and disease. *FASEB J.*, **17**, 1195–1214.
3. Henle,E.S. and Linn,S. (1997) Formation, prevention, and repair of DNA damage by iron hydrogen peroxide. *J. Biol. Chem.*, **272**, 19095–19098.
4. Wagner,J.R., Hu,C.C. and Ames,B.N. (1992) Endogenous oxidative damage of deoxycytidine in DNA. *Proc. Natl Acad. Sci. USA*, **89**, 3380–3384.
5. Kreutzer,D.A. and Essigmann,J.M. (1998) Oxidized, deaminated cytosines are a source of C -> T transitions *in vivo*. *Proc. Natl Acad. Sci. USA*, **95**, 3578–3582.
6. Wang,D., Kreutzer,D.A. and Essigmann,J.M. (1998) Mutagenicity and repair of oxidative DNA damage: insights from studies using defined lesions. *Mutat. Res.*, **400**, 99–115.
7. Razin,A. and Riggs,A.D. (1980) DNA methylation and gene-function. *Science*, **210**, 604–610.
8. Ehrlich,M., Gamasosa,M.A., Huang,L.H., Midgett,R.M., Kuo,K.C., McCune,R.A. and Gehrke,C. (1982) Amount and distribution of 5-methylcytosine in human DNA from different types of tissues or cells. *Nucleic Acids Res.*, **10**, 2709–2721.
9. Pfeifer,G.P. (2000) p53 mutational spectra and the role of methylated CpG sequences. *Mutat. Res.*, **450**, 155–166.
10. Lee,D.H., O'Connor,T.R. and Pfeifer,G.P. (2002) Oxidative DNA damage induced by copper and hydrogen peroxide promotes CG->TT tandem mutations at methylated CpG dinucleotides in nucleotide excision repair-deficient cells. *Nucleic Acids Res.*, **30**, 3566–3573.
11. Zhang,Q. and Wang,Y. (2003) Independent generation of 5-(2′-deoxycytidinyl)methyl radical and the formation of a novel cross-link lesion between 5-methylcytosine and guanine. *J. Am. Chem. Soc.*, **125**, 12795–12802.
12. Zhang,Q. and Wang,Y. (2005) Generation of 5-(2′-deoxycytidyl)-methyl radical and the formation of intrastrand cross-link lesions in oligodeoxyribonucleotides. *Nucleic Acids Res.*, **33**, 1593–1603.
13. Gu,C. and Wang,Y. (2004) LC-MS/MS identification and yeast polymerase η bypass of a novel γ-irradiation-induced intrastrand cross-link lesion G[8-5]C. *Biochemistry*, **43**, 6745–6750.
14. Box,H.C., Budzinski,E.E., Dawidzik,J.B., Wallace,J.C. and Iijima,H. (1998) Tandem lesions and other products in X-irradiated DNA oligomers. *Radiat. Res.*, **149**, 433–439.
15. Box,H.C., Budzinski,E.E., Dawidzik,J.B., Gobey,J.S. and Freund,H.G. (1997) Free radical-induced tandem base damage in DNA oligomers. *Free Radic. Biol. Med.*, **23**, 1021–1030.
16. Romieu,A., Bellon,S., Gasparutto,D. and Cadet,J. (2000) Synthesis and UV photolysis of oligodeoxynucleotides that contain 5-(phenylthiomethyl)-2′-deoxyuridine: a specific photolabile precursor of 5-(2′-deoxyuridilyl)methyl radical. *Org. Lett.*, **2**, 1085–1088.
17. Bellon,S., Ravanat,J.L., Gasparutto,D. and Cadet,J. (2002) Cross-linked thymine-purine base tandem lesions: synthesis, characterization, and measurement in gamma-irradiated isolated DNA. *Chem. Res. Toxicol.*, **15**, 598–606.
18. Zhang,Q. and Wang,Y. (2004) Independent generation of the 5-hydroxy-5,6-dihydrothymidin-6-yl radical and its reactivity in dinucleoside monophosphates. *J. Am. Chem. Soc.*, **126**, 13287–13297.
19. Zeng,Y. and Wang,Y. (2004) Facile formation of an intrastrand cross-link lesion between cytosine and guanine upon pyrex-filtered UV light irradiation of d(^{Br}CG) and duplex DNA containing 5-bromocytosine. *J. Am. Chem. Soc.*, **126**, 6552–6553.
20. Agarwal,K., Sharma,A. and Talukder,G. (1989) Effects of copper on mammalian cell components. *Chem. Biol. Interact.*, **69**, 1–16.
21. Lewis,C.D. and Laemmli,U.K. (1982) Higher order metaphase chromosome structure: evidence for metalloprotein interactions. *Cell*, **29**, 171–181.
22. Chevion,M. (1988) A site-specific mechanism for free radical induced biological damage: the essential role of redox-active transition metals. *Free Radic. Biol. Med.*, **5**, 27–37.
23. Aruoma,O.I., Halliwell,B., Gajewski,E. and Dizdaroglu,M. (1991) Copper-ion-dependent damage to the bases in DNA in the presence of hydrogen peroxide. *Biochem. J.*, **273**, 601–604.
24. Liang,Q. and Dedon,P.C. (2001) Cu(II)/H$_2$O$_2$-induced DNA damage is enhanced by packaging of DNA as a nucleosome. *Chem. Res. Toxicol.*, **14**, 416–422.
25. Drouin,R., Rodriguez,H., Gao,S.W., Gebreyes,Z., O'Connor,T.R., Holmquist,G.P. and Akman,S.A. (1996) Cupric ion/ascorbate/hydrogen peroxide-induced DNA damage: DNA-bound copper ion primarily induces base modifications. *Free Radic. Biol. Med.*, **21**, 261–273.
26. Tachon,P. (1989) Ferric and cupric ions requirement for DNA single-strand breakage by H$_2$O$_2$. *Free Radic. Res. Commun.*, **7**, 1–10.
27. Dizdaroglu,M., Rao,G., Halliwell,B. and Gajewski,E. (1991) Damage to the DNA bases in mammalian chromatin by hydrogen peroxide in the presence of ferric and cupric ions. *Arch. Biochem. Biophys.*, **285**, 317–324.
28. Barbouti,A., Doulias,P.T., Zhu,B.Z., Frei,B. and Galaris,D. (2001) Intracellular iron, but not copper, plays a critical role in hydrogen peroxide-induced DNA damage. *Free Radic. Biol. Med.*, **31**, 490–498.
29. Randerath,K., Reddy,M.V. and Disher,R.M. (1986) Age- and tissue-related DNA modifications in untreated rats: detection by ^{32}P-postlabeling assay and possible significance for spontaneous tumor induction and aging. *Carcinogenesis*, **7**, 1615–1617.
30. Randerath,K., Yang,P.F., Danna,T.F., Reddy,R., Watson,W.P. and Randerath,E. (1991) Bulky adducts detected by ^{32}P-postlabeling in DNA modified by oxidative damage in vitro. Comparison with rat lung I-compounds. *Mutat. Res.*, **250**, 135–144.
31. Randerath,E., Watson,W.P., Zhou,G.D., Chang,J. and Randerath,K. (1995) Intensification and depletion of specific bulky renal DNA adducts (I-compounds) following exposure of male F344 rats to the renal carcinogen ferric nitrilotriacetate (Fe-NTA). *Mutat. Res.*, **341**, 265–279.
32. Randerath,K., Randerath,E., Smith,C.V. and Chang,J. (1996) Structural origins of bulky oxidative DNA adducts (type II I-compounds) as deduced by oxidation of oligonucleotides of known sequence. *Chem. Res. Toxicol.*, **9**, 247–254.
33. Randerath,K., Randerath,E., Zhou,G.D. and Li,D. (1999) Bulky endogenous DNA modifications (I-compounds) -possible structural origins and functional implications. *Mutat. Res.*, **424**, 183–194.
34. Carmichael,P.L., She,M.N. and Phillips,D.H. (1992) Detection and characterization by ^{32}P-postlabelling of DNA adducts induced by a Fenton-type oxygen radical-generating system. *Carcinogenesis*, **13**, 1127–1135.
35. Chang,J., Watson,W.P., Randerath,E. and Randerath,K. (1993) Bulky DNA-adduct formation induced by Ni(II) in vitro and in vivo as assayed by ^{32}P-postlabeling. *Mutat. Res.*, **291**, 147–159.
36. Randerath,K., Zhou,G.D., Somers,R.L., Robbins,J.H. and Brooks,P.J. (2001) A ^{32}P-postlabeling assay for the oxidative DNA lesion 8,5′-cyclo-2′-deoxyadenosine in mammalian tissues: evidence that four type II I-compounds are dinucleotides containing the lesion in the 3′ nucleotide. *J. Biol. Chem.*, **276**, 36051–36057.
37. Lloyd,D.R., Phillips,D.H. and Carmichael,P.L. (1997) Generation of putative intrastrand cross-links and strand breaks in DNA by transition metal ion-mediated oxygen radical attack. *Chem. Res. Toxicol.*, **10**, 393–400.
38. Lloyd,D.R. and Phillips,D.H. (1999) Oxidative DNA damage mediated by copper(II), iron(II) and nickel(II) Fenton reactions: evidence for site-specific mechanisms in the formation of double-strand breaks, 8-hydroxydeoxyguanosine and putative intrastrand cross-links. *Mutat. Res.*, **424**, 23–36.
39. Hong,H., Cao,H., Wang,Y. and Wang,Y. (2006) Identification and quantification of a guanine-thymine intrastrand cross-link lesion

induced by Cu(II)/H_2O_2/ascorbate. *Chem. Res. Toxicol.*, **19**, 614–621.

40. LaFrancois,C.J., Fujimoto,J. and Sowers,L.C. (1998) Synthesis and characterization of isotopically enriched pyrimidine deoxynucleoside oxidation damage products. *Chem. Res. Toxicol.*, **11**, 75–83.

41. Frelon,S., Douki,T., Ravanat,J.L., Pouget,J.P., Tornabene,C. and Cadet,J. (2000) High-performance liquid chromatography-tandem mass spectrometry measurement of radiation-induced base damage to isolated and cellular DNA. *Chem. Res. Toxicol.*, **13**, 1002–1010.

42. Zeng,Y. and Wang,Y. (2006) Sequence-dependent formation of intrastrand crosslink products from the UVB irradiation of duplex DNA containing a 5-bromo-2'-deoxyuridine or 5-bromo-2'-deoxycytidine. *Nucleic Acids Res.*, **34**, 6521–6529.

43. Hong,H. and Wang,Y. (2005) Formation of intrastrand cross-link products between cytosine and adenine from UV irradiation of d(^{Br}CA) and duplex DNA containing a 5-bromocytosine. *J. Am. Chem. Soc.*, **127**, 13969–13977.

44. von Sonntag,C. (1987) *The Chemical Basis of Radiation Biology*. Taylor & Francis, London.

45. Behe,M. and Felsenfeld,G. (1981) Effects of methylation on a synthetic polynucleotide: The B-Z transition in poly(dG-m^{5}dC).poly(dG-m^{5}dC). *Proc. Natl Acad. Sci. USA*, **78**, 1619–1623.

46. Gu,C. and Wang,Y. (2005) Thermodynamic and in vitro replication studies of an intrastrand G[8-5]C cross-link lesion. *Biochemistry*, **44**, 8883–8889.

47. Gu,C., Zhang,Q., Yang,Z., Wang,Y., Zou,Y. and Wang,Y. (2006) Recognition and incision of oxidative intrastrand cross-link lesions by UvrABC nuclease. *Biochemistry*, **45**, 10739–10746.

48. Bellon,S., Gasparutto,D., Saint-Pierre,C. and Cadet,J. (2006) Guanine-thymine intrastrand cross-linked lesion containing oligo-nucleotides: from chemical synthesis to in vitro enzymatic replica-tion. *Org. Biomol. Chem.*, **4**, 3831–3837.

49. Yang,Z., Colis,L.C., Basu,A.K. and Zou,Y. (2005) Recognition and incision of gamma-radiation-induced cross-linked guanine-thymine tandem lesion G[8,5-Me]T by UvrABC nuclease. *Chem. Res. Toxicol.*, **18**, 1339–1346.

50. Reardon,J.T., Bessho,T., Kung,H.C., Bolton,P.H. and Sancar,A. (1997) *In vitro* repair of oxidative DNA damage by human nucleotide excision repair system: Possible explanation for neurodegeneration in Xeroderma pigmentosum patients. *Proc. Natl Acad. Sci. USA*, **94**, 9463–9468.

51. Berneburg,M. and Lehmann,A.R. (2001) Xeroderma pigmentosum and related disorders: defects in DNA repair and transcription. *Adv. Genet.*, **43**, 71–102.

52. Tremblay,S., Douki,T., Cadet,J. and Wagner,J.R. (1999) 2'-deoxycytidine glycols, a missing link in the free radical-mediated oxidation of DNA. *J. Biol. Chem.*, **274**, 20833–20838.

53. Zuo,S.J., Boorstein,R.J. and Teebor,G.W. (1995) Oxidative damage to 5-methylcytosine in DNA. *Nucleic Acids Res.*, **23**, 3239–3243.

54. Burdzy,A., Noyes,K.T., Valinluck,V. and Sowers,L.C. (2002) Synthesis of stable-isotope enriched 5-methylpyrimidines and their use as probes of base reactivity in DNA. *Nucleic Acids Res.*, **30**, 4068–4074.

55. Rideout,W.M., Coetzee,G.A., Olumi,A.F. and Jones,P.A. (1990) 5-Methylcytosine as an endogenous mutagen in the human LDL receptor and p53 genes. *Science*, **249**, 1288–1290.

56. Kamiya,H., Tsuchiya,H., Karino,N., Ueno,Y., Matsuda,A. and Harashima,H. (2002) Mutagenicity of 5-formylcytosine, an oxida-tion product of 5-methylcytosine, in DNA in mammalian cells. *J. Biochem.*, **132**, 551–555.

57. Klose,R.J. and Bird,A.P. (2006) Genomic DNA methylation: the mark and its mediators. *Trends Biochem. Sci.*, **31**, 89–97.

58. Valinluck,V., Tsai,H.H., Rogstad,D.K., Burdzy,A., Bird,A. and Sowers,L.C. (2004) Oxidative damage to methyl-CpG sequences inhibits the binding of the methyl-CpG binding domain (MBD) of methyl-CpG binding protein 2 (MeCP2). *Nucleic Acids Res.*, **32**, 4100–4108.

59. Turk,P.W., Laayoun,A., Steven,S.S. and Weitzman,S.A. (1995) DNA adduct 8-hydroxyl-2'-deoxyguanosine (8-hydroxyguanine) affects function of human DNA methyltransferase. *Carcinogenesis*, **16**, 1253–1255.

60. Valinluck,V. and Sowers,L.C. (2007) Endogenous cytosine damage products alter the site selectivity of human DNA maintenance methyltransferase DNMT1. *Cancer Res.*, **67**, 946–950.

61. Reif,D.W. (1992) Ferritin as a source of iron for oxidative damage. *Free Radic. Biol. Med.*, **12**, 417–427.

62. Calderaro,M., Martins,E.A.L. and Meneghini,R. (1993) Oxidative stress by menadione affects cellular copper and iron homeostasis. *Mol. Cell. Biochem.*, **126**, 17–23.

63. Abalea,V., Cillard,J., Dubos,M.P., Anger,J.P., Cillard,P. and Morel,I. (1998) Iron-induced oxidative DNA damage and its repair in primary rat hepatocyte culture. *Carcinogenesis*, **19**, 1053–1059.

64. Toyokuni,S. (1996) Iron-induced carcinogenesis: The role of redox regulation. *Free Radic. Biol. Med.*, **20**, 553–566.

65. Carmichael,P.L., Hewer,A., Osborne,M.R., Strain,A.J. and Phillips,D.H. (1995) Detection of bulky DNA lesions in the liver of patients with Wilson's disease and primary hemochromatosis. *Mutat. Res.*, **326**, 235–243.